

Supporting information

NiO-MgO prepared by the complex-decomposition method as a catalyst for carbon dioxide reforming of methane

Ying Wang, Bin Li, Yong-Shan Xiao, Zhong-Wen Liu*

*Key Laboratory of Syngas Conversion of Shaanxi Province, School of Chemistry and Chemical
Engineering, Shaanxi Normal University, Xi'an 710119, China*

* Correspondence: zwliu@snnu.edu.cn

No. 620, West Chang'an Avenue

School of Chemistry & Chemical Engineering

Shaanxi Normal University

Xi'an 710119, China

Tel: +86-29-8153-0801

Fax: +86-29-8153-0727

E-mail: zwliu@snnu.edu.cn

List of contents

Figure S1. N ₂ adsorption-desorption isotherms of the fresh Ni _{0.1} Mg _{0.9} O-800-Y catalysts.....	3
Figure S2. TEM images of the reduced Ni _{0.1} Mg _{0.9} O-800-Y catalysts.....	4
Figure S3. XRD patterns of the fresh and reduced Ni _{0.1} Mg _{0.9} O-Gly-T catalysts.....	5
Figure S4. CH ₄ conversions of Ni _{0.1} Mg _{0.9} O-T-Gly and Ni _x Mg _{1-x} O-800-Gly catalysts.....	6
Figure S5. XRD patterns of the fresh and reduced Ni _x Mg _{1-x} O-800-Gly catalysts.....	7
Figure S6. TG curves and XRD patterns of the spent Ni _{0.1} Mg _{0.9} O-T-Gly catalysts.....	8
Figure S7. TG curves and XRD patterns of the spent Ni _x Mg _{1-x} O-800-Gly catalysts.....	9
Table S1 Summarized reaction conditions and the typical CRM results of the optimal NiO-MgO and the representatively reported Ni-based catalysts.....	10

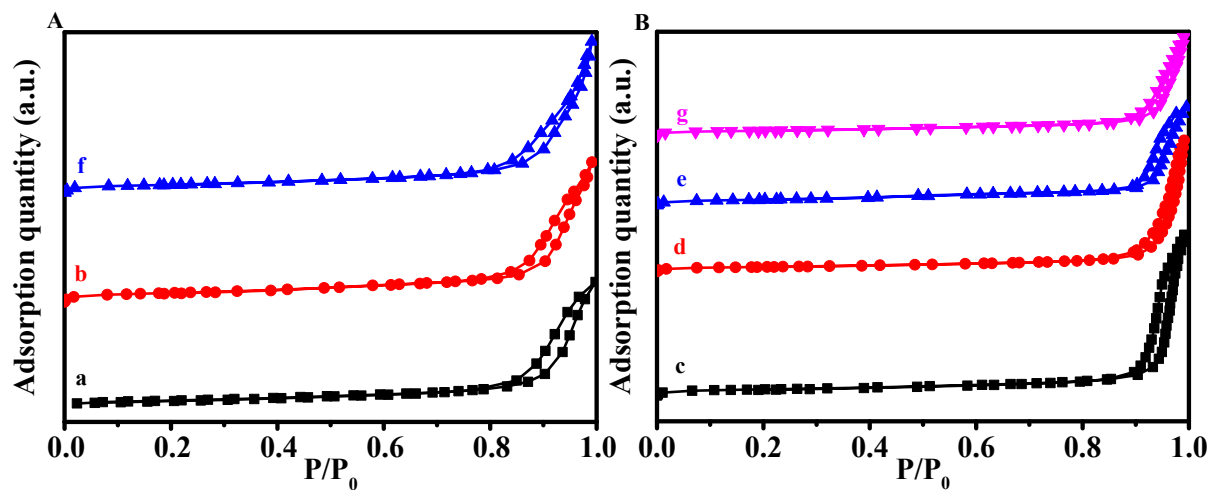


Figure S1. N₂ adsorption-desorption isotherms of the fresh catalysts of Ni_{0.1}Mg_{0.9}O-800-Gly (a), Ni_{0.1}Mg_{0.9}O-800-Gla (b), Ni_{0.1}Mg_{0.9}O-800-Oxa (c), Ni_{0.1}Mg_{0.9}O-800-Pro (d), Ni_{0.1}Mg_{0.9}O-800-Ser (e), Ni_{0.1}Mg_{0.9}O-800-Urea (f), and Ni_{0.1}Mg_{0.9}O-800-Ala (g).

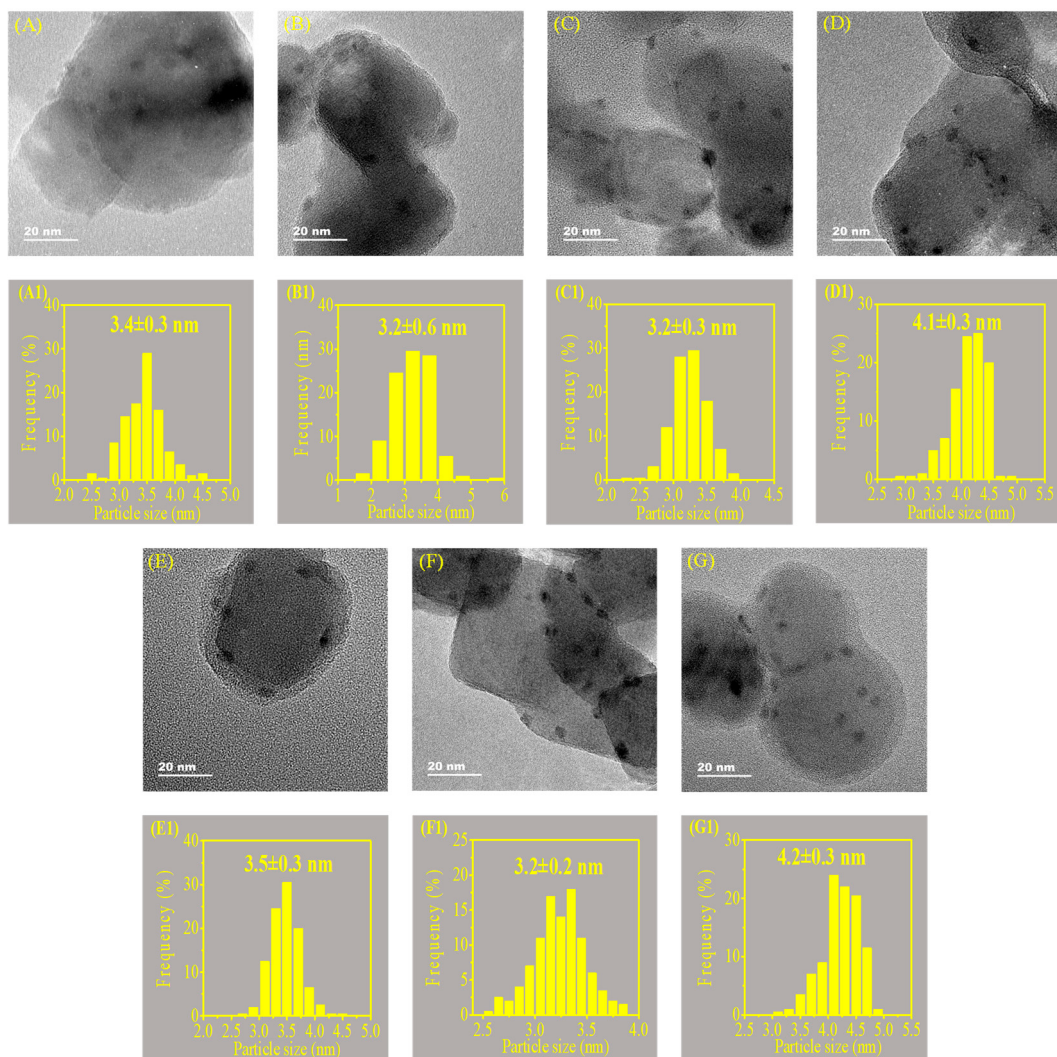


Figure S2. TEM images and the corresponding particle-size distributions for the reduced catalysts of $\text{Ni}_{0.1}\text{Mg}_{0.9}\text{O-800-Gly}$ (A, A1), $\text{Ni}_{0.1}\text{Mg}_{0.9}\text{O-800-Gla}$ (B, B1), $\text{Ni}_{0.1}\text{Mg}_{0.9}\text{O-800-Oxa}$ (C, C1), $\text{Ni}_{0.1}\text{Mg}_{0.9}\text{O-800-Pro}$ (D, D1), $\text{Ni}_{0.1}\text{Mg}_{0.9}\text{O-800-Ser}$ (E, E1), $\text{Ni}_{0.1}\text{Mg}_{0.9}\text{O-800-Urea}$ (F, F1), $\text{Ni}_{0.1}\text{Mg}_{0.9}\text{O-800-Ala}$ (G, G1).

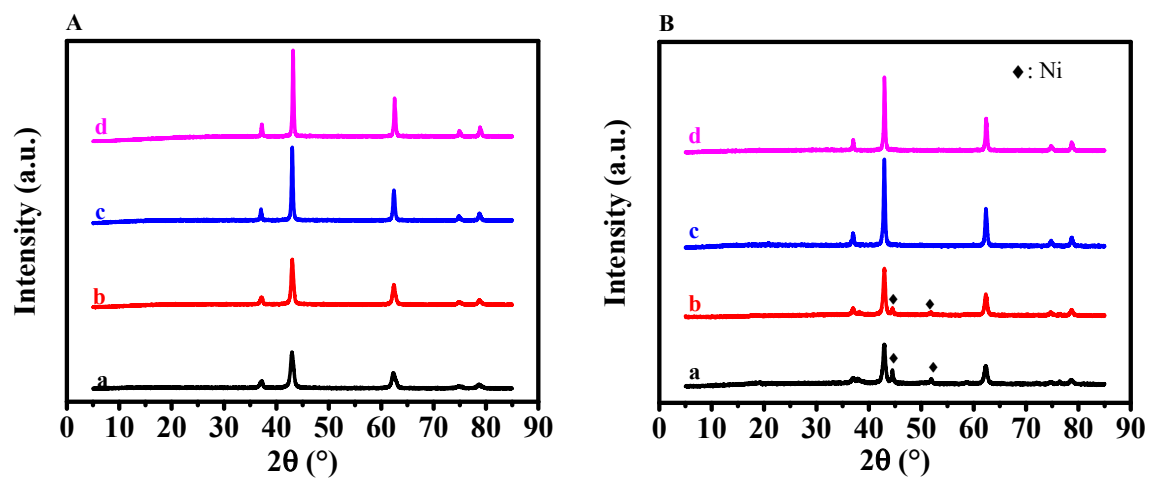


Figure S3. XRD patterns for the fresh (A) and reduced (B) catalysts of $\text{Ni}_{0.1}\text{Mg}_{0.9}\text{O}$ -Gly-600 (a), $\text{Ni}_{0.1}\text{Mg}_{0.9}\text{O}$ -Gly-700 (b), $\text{Ni}_{0.1}\text{Mg}_{0.9}\text{O}$ -Gly-800 (c), $\text{Ni}_{0.1}\text{Mg}_{0.9}\text{O}$ -Gly-900 (d).

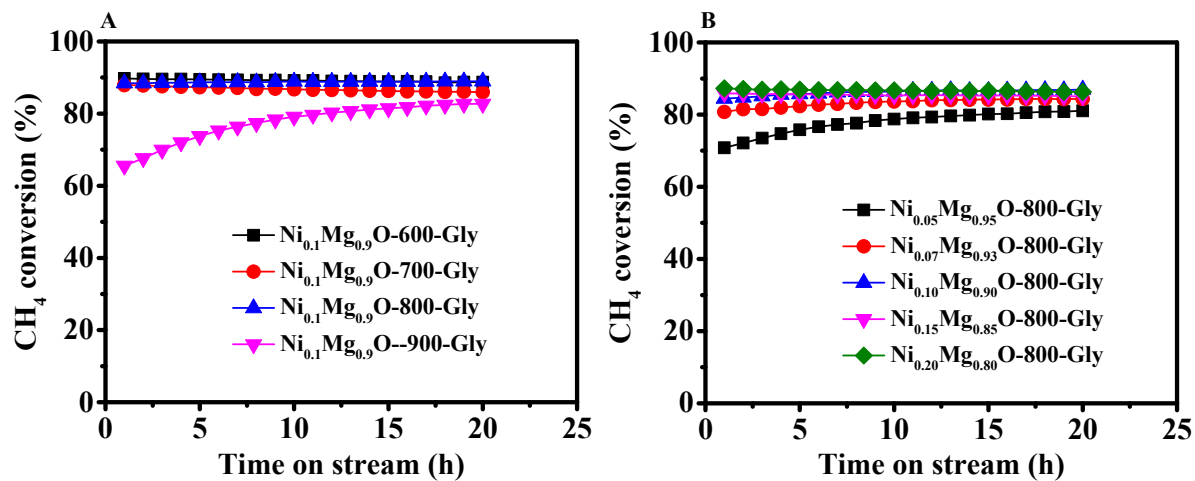


Figure S4. The time-on-stream conversions of CH₄ for Ni_{0.1}Mg_{0.9}O-T-Gly (A) and Ni_xMg_{1-x}O-800-Gly (B) catalyzed CRM under the conditions of CH₄/CO₂ = 1, 750 °C, 0.1 MPa and GHSV of 60000 mL·g⁻¹·h⁻¹

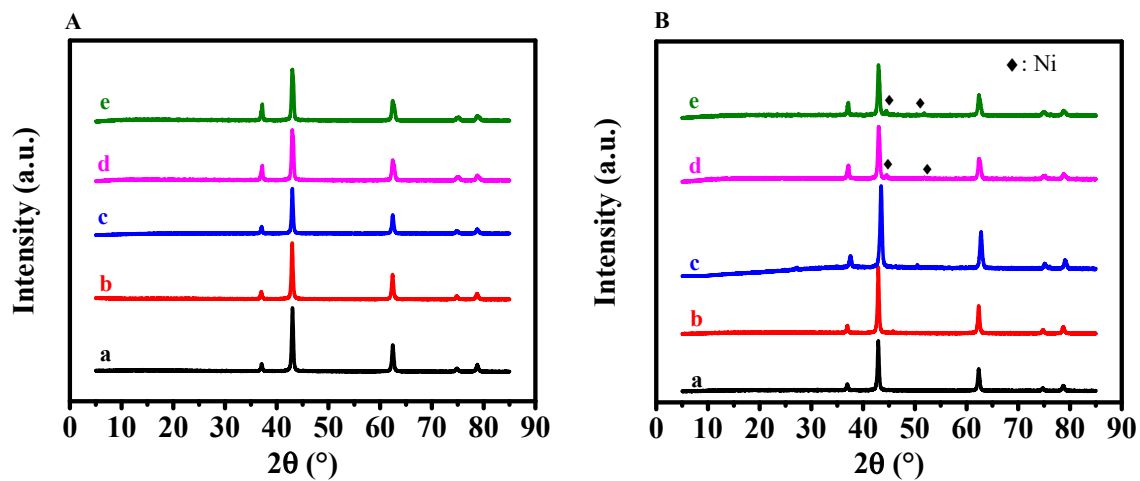


Figure S5. XRD patterns of fresh (A) and reduced (B) catalysts of $\text{Ni}_{0.05}\text{Mg}_{0.95}\text{O-800-Gly}$ (a), $\text{Ni}_{0.07}\text{Mg}_{0.93}\text{O-800-Gly}$ (b), $\text{Ni}_{0.10}\text{Mg}_{0.90}\text{O-800-Gly}$ (c), $\text{Ni}_{0.15}\text{Mg}_{0.85}\text{O-800-Gly}$ (d), $\text{Ni}_{0.20}\text{Mg}_{0.80}\text{O-800-Gly}$ (e).

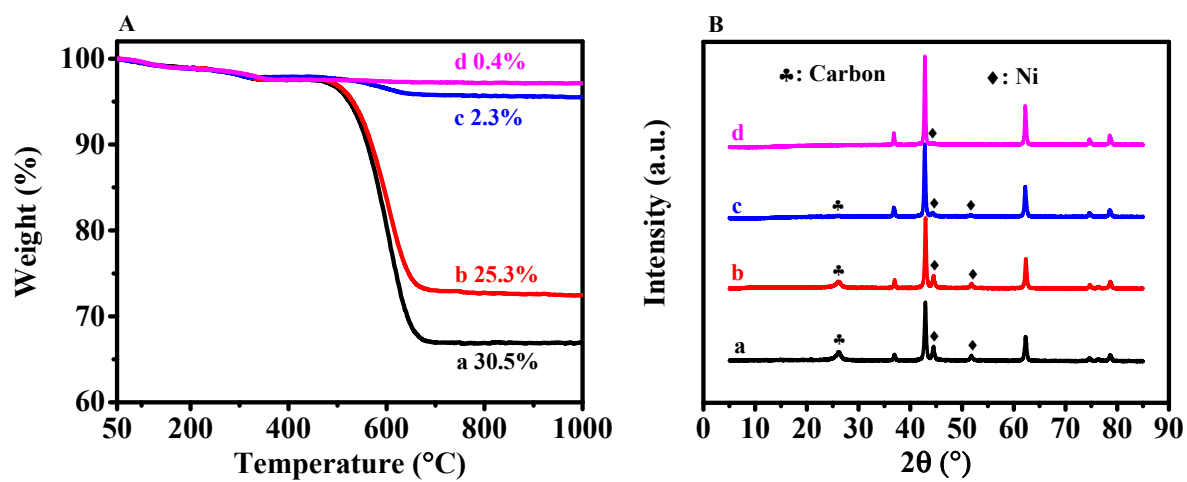


Figure S6. TG curves (A) and XRD patterns (B) for the spent catalysts of $\text{Ni}_{0.1}\text{Mg}_{0.9}\text{O-Gly-600}$ (a), $\text{Ni}_{0.1}\text{Mg}_{0.9}\text{O-Gly-700}$ (b), $\text{Ni}_{0.1}\text{Mg}_{0.9}\text{O-Gly-800}$ (c), $\text{Ni}_{0.1}\text{Mg}_{0.9}\text{O-Gly-900}$ (d).

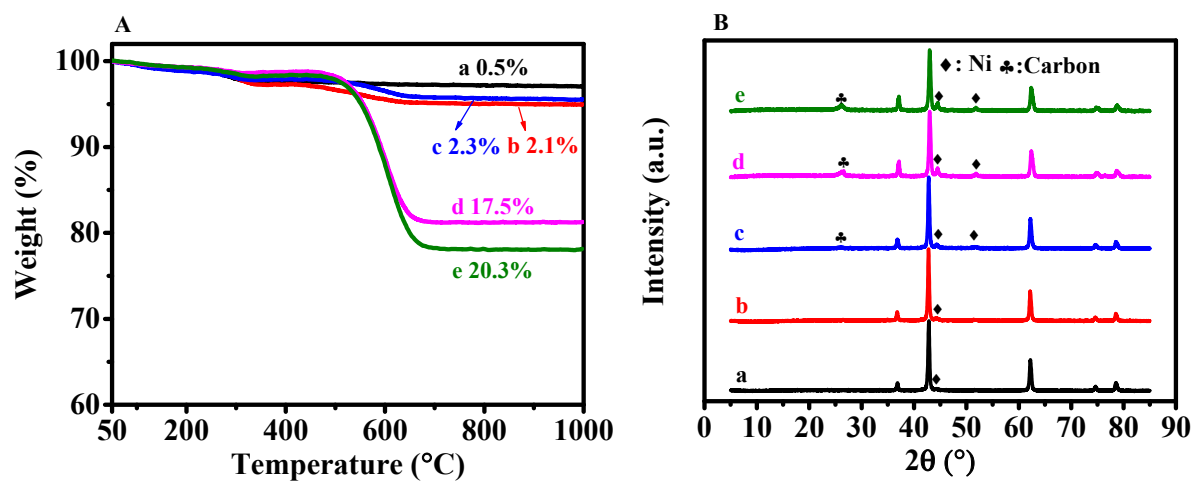


Figure S7. TG curves (A) and XRD patterns (B) for the spent catalysts of Ni_{0.05}Mg_{0.95}O-800-Gly (a), Ni_{0.07}Mg_{0.93}O-800-Gly (b), Ni_{0.10}Mg_{0.90}O-800-Gly (c), Ni_{0.15}Mg_{0.85}O-800-Gly (d), Ni_{0.20}Mg_{0.80}O-800-Gly (e).

Table S1 Summarized reaction conditions and the typical CRM results of the optimal NiO-MgO and the representatively reported Ni-based catalysts.

Catalysts	Temperature (°C)	Feed molar ratio	GHSV ($\times 10^4$ mL \cdot h $^{-1}$ \cdot g $^{-1}$)	Activity (mol \cdot g $^{-1}$ \cdot h $^{-1}$)*	Stability (%/h)*	References
Ni _{0.1} Mg _{0.9} O-800-Gly	750	CH ₄ /CO ₂ = 1/1	6.0	11.5	0	This work
Ni/MOR zeolite	650	CH ₄ /CO ₂ = 1/1	7.2	7.4	0.58	S1
Ni/SBA-15	750	CH ₄ /CO ₂ /N ₂ = 1/1/2	1.2	11.4	0	S2
Ni/Al ₂ O ₃ -Ole	800	CH ₄ /CO ₂ /N ₂ = 1/1/1	2.4	~ 3.2	0	S3
Pt-12Ni/hydrotalcite	700	CH ₄ /CO ₂ /Ar = 2/2/1	18	~ 42.2	0.13	S4
Ni/La ₂ O ₂ CO ₃ -Al ₂ O ₃	650	CH ₄ /CO ₂ /N ₂ = 3/3/14	24	~ 20.9	0	S5
Ni/Al ₂ O ₃	700	CH ₄ /CO ₂ = 1/1	3.0	8.1	0	S6

*: The specific activity is defined as CH₄ converted per gram of Ni over the loaded catalyst per hour, and the stability is estimated by the average rate for the decrease of CH₄ conversion with increasing the time on stream.

References

- S1** Bacariza, C.; Karam, L.; Hassan, N.E.; Lopes, J.M.; Henriques, C. Carbon dioxide reforming of methane over nickel-supported zeolites: a screening study. *Processes*. **2022**, *10*, 1331
- S2** Park, K.S.; Cho, J.M.; Park, Y.M.; Kwon, J.H.; Yu, J.S.; Jeong, H.E.; Choung, J.W.; Bae J.W., Enhanced thermal stability of Ni nanoparticles in ordered mesoporous supports for dry reforming of methane with CO₂. *Catal. Today* **2022**, 388-389, 224-230.
- S3** Seo, J.-C.; Kim, H.; Lee, Y.-L.; Nam, S.; Roh, H.-S. Lee, K.; Park, S.B., One-pot synthesis of full-featured mesoporous Ni/Al₂O₃ catalysts via pyrolysis-assisted evaporation-induced self-assembly method for dry reforming of methane. *ACS Sustainable Chem. Eng.* **2021**, *9*, 894-904.
- S4** Niu, J.; Wang, Y.; Liland, S.E.; Regli, S.K.; Yang, J.; Rout, K.R.; Luo, J.; Ronning, M.; Ran, J.; Chen D. Unraveling enhanced activity, selectivity, and coke resistance of Pt-Ni bimetallic clusters in dry reforming. *ACS Catal.* **2021**, *11*, 2398-2411.
- S5** Li, K.; Pei, C. Li, X.; Chen, S.; Zhang, X.; Liu, R.; Gong, J. Dry reforming of methane over La₂O₂CO₃-modified Ni/Al₂O₃ catalysts with moderate metal support interaction. *Appl. Catal. B-Environ.* **2020**, *264*, 118448.
- S6** Ma, Q.; Han, Y.; Wei, Q.; Makpal S.; Gao, X.; Zhang, J.; Zhao, T.-S., Stabilizing Ni on bimodal mesoporous-macroporous alumina with enhanced coke tolerance in dry reforming of methane to syngas. *J. CO₂ Util.* **2020**, *35*, 288-297.